Bioresource Technology 318 (2020) 123921

Contents lists available at ScienceDirect

Bioresource Technology

journal homepage: www.elsevier.com/locate/biortech

Short Communication

Impact of external resistance acclimation on charge transfer and diffusion resistance in bench-scale microbial fuel cells

Ruggero Rossi, Bruce E. Logan*

Department of Civil and Environmental Engineering, Penn State University, University Park, PA 16802, USA

ARTICLE INFO

Keywords:
Electrochemical impedance spectroscopy
Microbial fuel cell
Anode resistance
Charge transfer
Diffusion resistance

ABSTRACT

Reducing the external resistance (R_{ext}) for microbial fuel cell (MFC) acclimation can substantially alter the anode performance in terms of charge transfer (R_{CT}), diffusion (R_d) and total anode resistance (R_{An}). Electrochemical impedance spectroscopy (EIS) was used to quantify anode impedance at different set potentials. Reducing R_{ext} from 50 Ω to 20 Ω during acclimation reduced R_{CT} by 31% (from 6.12 ± 0.09 mΩ m^2 to 4.21 ± 0.03 mΩ m^2) and R_d by 18% (from 3.4 ± 0.2 mΩ m^2 to 2.8 ± 0.1 mΩ m^2) at a set anode potential of −115 mV during EIS. Overall R_{An} decreased by 27%, to 5.13 ± 0.02 mΩ m^2 for acclimation at 20 Ω, enabling the anode to achieve 38% higher current densities of 29 ± 1 A m^{-2}. The results show a clear dependence of acclimation procedures and external resistance on kinetic and diffusion components of anode impedance that can impact overall bioelectrochemical performance.

1. Introduction

The microbial anode is the key-component of microbial fuel cells (MFCs), producing electrons from organic matter oxidation of compounds in solution by exoelectrogenic bacteria colonizing the electrode (Logan, 2009; Logan et al., 2019). Electrons generated at the anode are consumed by the oxygen reduction reaction (ORR) at the cathode, where oxygen is reduced to hydroxide ions in an aqueous environment (Popat et al., 2012; Torres et al., 2008). With a low external resistance (R_{ext}) MFCs can produce higher current densities and thus the microorganisms on the anode will more rapidly oxidize the substrate (Lyon et al., 2010; Zhang et al., 2015). However, for every molecule of acetate oxidized, eight protons are released into solution from the biofilm on the electrode. If protons are not effectively combined with the buffer ions, their accumulation can lead to the acidification of the biofilm, reducing the viability of the exoelectrogenic bacteria and limiting the maximum current generation and therefore the performance of the MFC (Bond et al., 2012; Torres et al., 2008). This decrease in pH and other factors such as buffer concentration or a set anode potential have been previously shown to alter the performance of the MFC (Torres et al., 2008; Zhu et al., 2013).

Varying the external resistance used in the external circuit of an MFC can produce many changes that can impact performance in terms of maximum power density (Hong et al., 2011), maximum current density (Zhu et al., 2013), and coulombic efficiency (Jung and Regan, 2011). For example, reducing R_{ext} from 5000 Ω to 500 Ω during acclimation increased the anodic peak current density from 3 A m^{-2} to 6 A m^{-2}, and further to 7 A m^{-2} for the lowest R_{ext} of 50 Ω. At the same time, the maximum power density based on polarization data increased from 700 mW m^{-2} to 1200 mW m^{-2} (Hong et al., 2011). Other studies have shown that varying the external resistance affects the anodic community, likely due to the adaptation of the microorganisms (Jung and Regan, 2011; Lyon et al., 2010). Changing R_{ext} also will likely change the anode potential and it has been shown that set potentials will influence the expression of different cytochromes by certain bacteria (Zhu et al., 2014). Moreover, reducing R_{ext} can increase the coulombic efficiency due to the higher current density produced by the reactor and shorter cycles for MFCs operated in fed batch mode (Jung and Regan, 2011; Zhang et al., 2015). Recent studies have shown that bioanode performance can be described by the individual contribution of the charge transfer (R_{CT}) and diffusion (R_d) resistances to the overall anode resistance (R_{An}) (Rossi et al., 2020). R_{CT} depends by the kinetic oxidation of acetate while R_d is due to diffusion of protons from the biofilm and the consequent acidification of the biofilm (Rossi and Logan, 2020; Rossi et al., 2020). However, there has been little attention given to the relative impact of the selected R_{ext} on the kinetic and mass-transfer components of the overall anode resistance.

In this study, the impact of the external resistance during acclimation was examined on the performance of the anode and the whole cell. By varying the external resistance, the current produced by the reactor

* Corresponding author.
E-mail address: blogan@psu.edu (B.E. Logan).

https://doi.org/10.1016/j.biortech.2020.123921
Received 7 July 2020; Received in revised form 23 July 2020; Accepted 24 July 2020
Available online 29 July 2020
0960-8524/

changes, with higher current densities produced at lower external resistances. The impact of the external resistance acclimation was investigated with respect to the overall anode resistance and the relative charge transfer and diffusion resistances using electrochemical impedance spectroscopy (EIS) as a function of different set potentials, and with linear sweep voltammetry (LSV) to determine the impact of the different acclimation resistances on the total anode resistance and maximum current densities.

2. Materials and methods

2.1. MFC materials, construction, and operation

MFCs were membrane-less, single-chamber 28 mL reactors with the graphite brush anode (2.5 cm × 2.5 cm) placed perpendicular to the cathode at a distance of ~1 cm. The brushes were heat treated (30 min.) at 450 °C in a muffle furnace before being used in the MFCs (Feng et al., 2010). Air cathodes with same projected area as the reactor cross-sectional area (7 cm^2) were purchased from VITO (Mol, Belgium).

Electrochemical tests were conducted in 50 mM PBS (PBS; 2.45 g L^{-1} NaH_2PO_4 H_2O, 4.58 g L^{-1} Na_2HPO_4, 0.31 g L^{-1} NH_4Cl, and 0.13 g L^{-1} KCl, conductivity of 6.93 mS $cm^{-1,}$ pH of 7.0 ± 0.1). The media contained sodium acetate 2 g L^{-1} and was amended with trace mineral and vitamin solutions (Cheng et al., 2009).

MFCs were operated in duplicate at 30 °C. The acclimation was conducted by inoculating the reactors with effluent from operating MFCs until at least three reproducible cycles were obtained. Thereafter, only fresh media was fed to the reactors in fed-batch mode with R_{ext} = 1000 Ω. Prior to electrochemical tests conducted here, the external resistance was reduced to 100 Ω, 50 Ω or 20 Ω for at least 10 h per day for two days while R_{ext} was increased by 500 Ω overnight to avoid acetate depletion that would have occurred with the lower external resistances (600 Ω, 550 Ω and 520 Ω overnight) (Watson and Logan, 2011). The external resistance was then reduced to either 100 Ω, 50 Ω or 20 Ω for at least 6 h prior to conducting any electrochemical tests on that day.

2.2. Electrochemical measurements

Electrochemical analyses of the brush anode (working electrode) were conducted using the cathode as the counter electrode and a Ag/AgCl reference electrode (RE) (Pine, NC; +199 mV vs a standard hydrogen electrode, SHE) as previously described (Rossi et al., 2020).

A quick EIS analysis conducted prior to the LSV (potential scanned from the open circuit potential (OCP) to +200 mV, 0.1 mV s^{-1} scan speed) was used to calculate the solution resistance (R_Ω) that was used for correcting the electrode potentials reported here (Logan et al., 2018). The electrode potentials, prior to being corrected for R_Ω are given in Supporting Information. The current and power density were calculated by normalizing to the cathode area of 7 cm^2.

The electrode resistances and experimental potentials were examined using the EPS method (Cario et al., 2019; Rossi et al., 2019) as previously described, and compared with results from EIS measurements. EIS spectra over a range of 100 × 10^6 mHz (100 kHz) to 5 mHz, with 5 mV amplitude perturbation and 10 pts/decade, were obtained at six anode potentials. Fitting of the spectra was accomplished with Zfit provided in the EC-lab software (Bio-Logic USA) to obtain numerical values of the electrochemical components of the equivalent circuits reported in the Supporting Information.

2.3. Calculations

In electrochemical processes where reaction rate is limited by mass-transfer, it is possible to determine, through EIS, the diffusion layer thickness as the zone of depletion around an electrode d, as

$$d = (D_{lim} t_{diff})^{1/2} \quad (1)$$

where D_{lim} is the diffusivity of the specific species limiting the process (H^+, 9.1 × 10^{-5} cm^2 s^{-1}) (Dykstra et al., 2014), and t_{diff} is the characteristic diffusion time calculated from the correspondent frequency (Bisquert et al., 1999).

The concentration of the chemical species (c_{lim}) responsible for the mass-transfer limited regime, diffusing through the diffusion layer was calculated (Bisquert et al., 1999) as:

$$c_{lim} = \frac{RTd}{z^2F^2D_{lim}R_d s} \quad (2)$$

where R is the gas constant (J mol^{-1} K^{-1}), T the temperature (K), F the Faraday constant (A s mol-e^{-1}), z the number of electrons produced by acetate oxidation (8) and s the effective electrode surface area (cm^2). The value of *s* was estimated by the double layer capacitance with the assumption that the specific capacitance of the flat carbon electrode was 10 μF cm^{-2} resulting in 8700 ± 2100 cm^2 (Zhou and Poorten, 1995). The capacitance of the anode was calculated assuming a Brug distribution (Brug et al., 1984; Dominguez-Benetton et al., 2012).

3. Results and discussion

3.1. Lowering R_{ext} reduced anodic charge transfer and diffusion resistance

To investigate the impact of the external resistance on the diffusion and charge transfer resistances, EIS spectra were obtained at six set electrode potentials ranging from −240 mV to −115 mV (Fig. 1) after MFCs were acclimated at external resistances of 50 Ω or 20 Ω. All the spectra showed a depressed semicircle at high frequencies (close to the origin). Applying a potential of −215 mV decreased the electrode impedance compared to −240 mV, as can be seen by the shift in the real part of the impedance toward the origin (Fig. 1). However, at applied potentials more positive than −240 mV a subsequent element was following the first semicircle, increasing the electrode impedance at low frequencies toward higher values. The first element has been identified with the charge transfer process (Q_{DL}/R_{CT}), linked to the bacterial oxidation of acetate. At electrode potentials more positive than −240 mV, the charge transfer was followed by a mass-transfer process ($Q_{DL}/R_{CT} + Z_d$) that had a magnitude that increased by increasing the current density and applying more positive potentials.

Fitting the spectra using the equivalent circuit reported in the Supporting Information enabled calculation of the individual charge transfer and diffusion resistances for anodes acclimated at 50 Ω and 20 Ω R_{ext} (Fig. 2). The charge transfer resistance represents the resistance to the kinetics of the electrochemically controlled reactions associated with the transfer of electrons. Favorable reactions have smaller R_{CT} and when a reaction is controlled only by kinetics, increasing the overpotentials usually reduces the charge transfer resistance. The charge transfer resistance with 50 Ω R_{ext} decreased by increasing the overpotential from 2.9 ± 0.4 mΩ m^2 (−240 mV) to 2.2 ± 0.3 mΩ m^2 (−215 mV). The initial decrease in R_{CT} suggested that the reaction was favored at higher potentials, typical of kinetically controlled electrochemical reactions. However, further increasing the anode potential led to an increase of R_{CT} to 6.1 ± 0.1 mΩ m^2 at the most positive potential of −115 mV. The increase in R_{CT} for both 50 Ω and 20 Ω R_{ext} at anode potentials higher than −215 mV was likely due to the adverse impact of diffusion on the anode kinetics.

When an electrochemical reaction is also controlled by mass-transfer processes, diffusion resistance increases the electrode resistance due to insufficient transport of either reactants to the electrode or products from the electrode. Applying more positive anode potentials increases current densities and therefore the relative impact of diffusion resistance to that of the charge transfer resistance. For example, R_d was only 0.4 ± 0.1 mΩ m^2 at an anode potential of −215 mV but it became more positive when increasing the anode

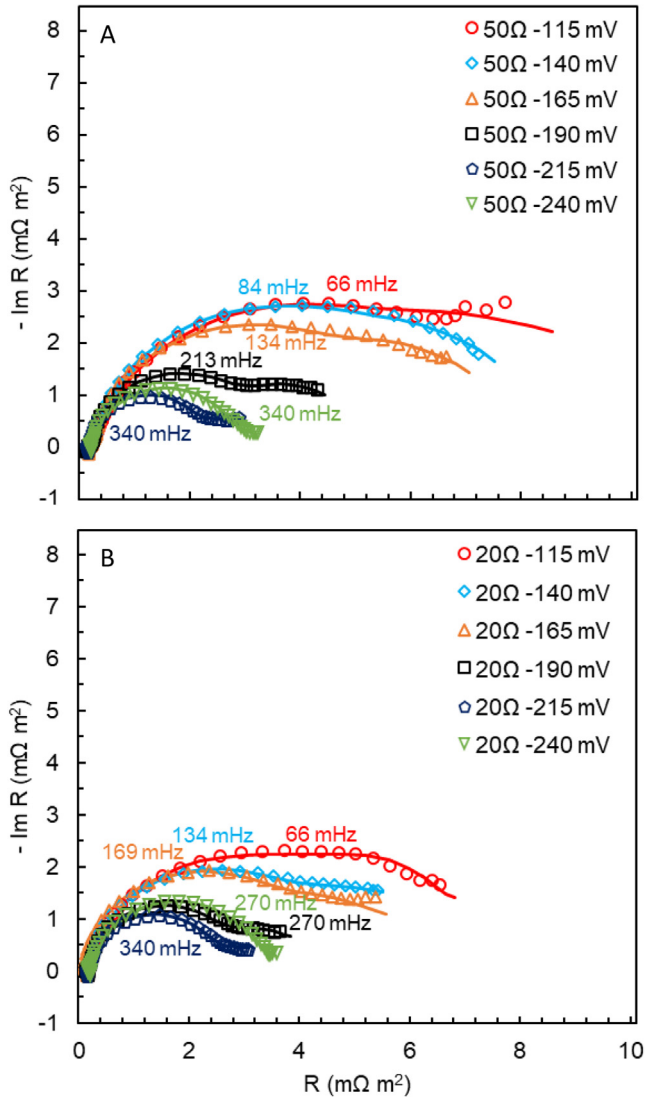

Fig. 1. EIS spectra of anodes acclimated at (A) 50 Ω and (B) 20 Ω external resistances. The numbers in mHz represent the characteristic frequencies that correspond to the maximum of the imaginary impedance. Fitting to the data are represented by solid lines. Duplicate spectra are shown in the Supporting Information.

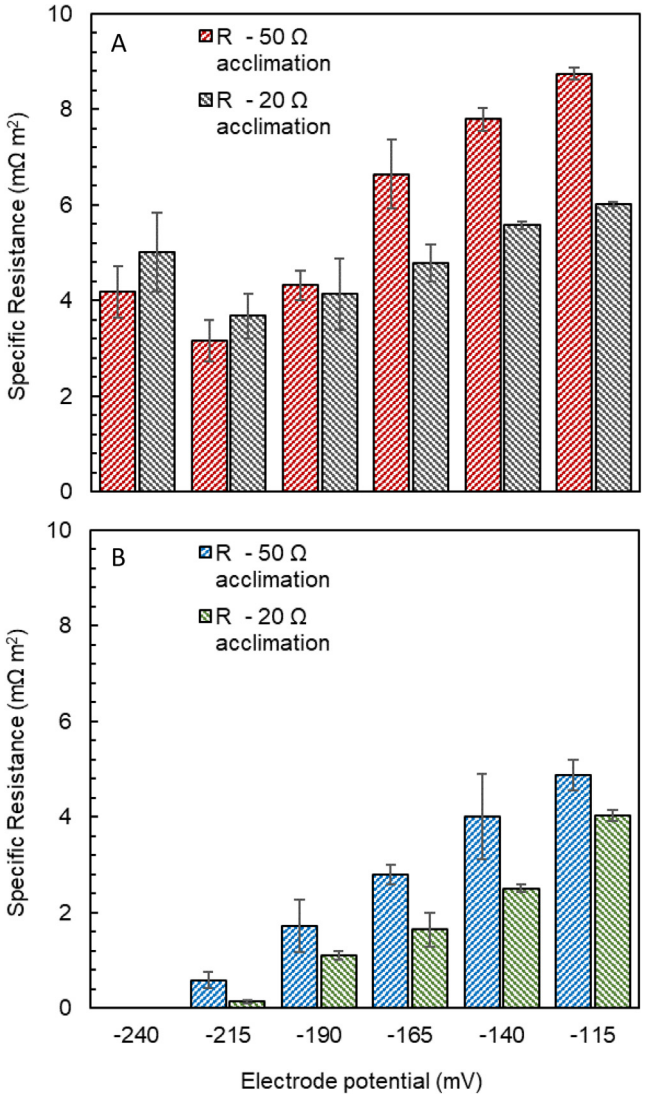

Fig. 2. Comparison of (A) charge transfer and (B) diffusion resistance of anodes acclimated with 50 Ω and 20 Ω external resistance.

potentials, reaching a maximum of 3.4 ± 0.2 mΩ m^2 at −115 mV with 50 Ω R_{ext}. Applying more positive potentials increased the magnitude of the R_d, further increasing the overall electrode resistance, and indicating that the diffusion of chemical species was limiting the rate of the electrochemical reaction.

The accumulation of protons at the anode can generate mass-transfer limitations that impact brush anode performance due to an insufficient rate of diffusion of protons from the anode relative to the rate of production of protons (Rossi et al., 2020). Using Eq. (2) the concentration of the chemical species limiting the electrochemical reaction was 0.18 μM, for conditions of 20 Ω R_{ext} and −215 mV. This concentration was similar to that of protons in 50 mM PBS at pH 7 (0.1 μM) suggesting that proton transport was a factor in the mass transfer resistance here. At the highest anode potential of −115 mV the concentration of the limiting species increased to 2.1 μM, corresponding to a proton concentration relative to a pH of 5.7. The diffusion layer represents a region over which the concentration of the chemical species responsible for the diffusion resistance changes from the surface concentration to the bulk concentration. The diffusion layer thickness, calculated with Eq. (1), indicated that protons were diffusing from the brush anode through a stagnant layer of 408 ± 8 μm. This diffusion layer was similar to that obtained with brush anodes in a previous study (Rossi et al., 2020).

The overall impact of reducing R_{ext} from 50 Ω to 20 Ω was to reduce charge transfer and diffusion resistances at more positive potentials. For example, at the most positive potential of −115 mV, R_{CT} at 20 Ω R_{ext} was 4.2 ± 0.0 mΩ m^2, 31% lower than that at 50 Ω (6.1 ± 0.1 m Ω m^2). The impact of the external resistance on diffusion resistance was smaller than that of the charge transfer resistance. R_d was 18% lower after acclimation with 20 Ω (2.8 ± 0.1 mΩ m^2) compared to that obtained after 50 Ω (3.4 ± 0.2 mΩ m^2) at the most positive potential of −115 mV. Operating the cell at low R_{ext} and higher current density can produce changes in the biofilm, for example generating a thicker biofilm (Zhu et al., 2014) and overexpression of cytochromes and proteins involved in the exogenous electron transfer (Yang et al., 2019), which could reduce charge transfer resistance. While it was suggested in one study that the response to different anode potentials was a change in the microbial composition of the anode (Torres et al., 2009) it was found in another study that there was no difference in anode communities operated at different set potentials (Zhu et al., 2014). Since R_d was primarily due to the accumulation of protons in the proximity of the anode surface, it is likely that variations in microbial activity at different pHs was the main factor in changes in the diffusion

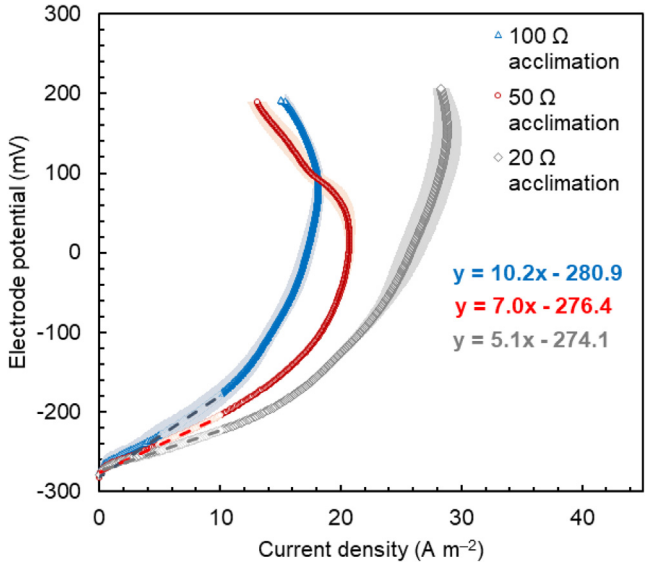

Fig. 3. LSVs of carbon brush anodes acclimated at different external resistances following corrections for R_{Ω}. Anode resistance was calculated from the linearized electrode potential over a current density range of 5–10 A m^{-2}.

resistances here.

3.2. Impact of external resistance acclimation on overall performance of the MFC

Reducing the external resistance during MFC acclimation improved the anode performance, with lower anode resistances and larger peak current densities, as shown in the LSVs (Fig. 3). Reducing R_{ext} from 100 Ω to 50 Ω decreased R_{An} by 31%, from 10.2 ± 0.1 mΩ m^2 to 7.0 ± 0.1 mΩ m^2 and by an additional 27% (R_{An} = 5.13 ± 0.02 m Ω m^2) by using a 20 Ω external resistance. The lower external resistances during acclimation showed a positive impact on the anode peak current density, with a 60% increase (from 18 A m^{-2} to 29 A m^{-2}) by reducing R_{ext} from 100 Ω to 20 Ω. The lower charge transfer and diffusion resistances obtained with an external resistance of 20 Ω (Fig. 2), with respect to that obtained using 50 Ω R_{ext}, provide an explanation for the lower R_{An} values obtained from these polarization curves (Fig. 3).

Varying the external resistance had a negligible impact on the cathode performance. R_{Cat} was 19.7 ± 0.3 mΩ m^2 at R_{ext} of 100 Ω and only slightly increased to 23.5 ± 0.5 mΩ m^2 at R_{ext} of 20 Ω. Despite the large variations in the anode resistances due to the lower acclimation resistances, the maximum power density increased by less than 5%, from 1766 ± 87 mW m^{-2} to 1850 ± 7 mW m^{-2}, when R_{ext} was decreased from 100 Ω to 20 Ω. This was likely due to the slight increase in R_{Cat} at the smaller R_{ext}, and the limited impact of the anode resistance on the overall internal resistance calculated from the slope of the polarization curves. For example, R_{An} accounted for ~26% of R_{int} at 100 Ω R_{ext}, and by ~14%, with 20 Ω R_{ext}, but R_{Cat} was ~51% (100 Ω) and ~64% (20 Ω) of the overall internal resistance.

3.3. Implications on reducing anode resistance with lower external resistances

Reducing the external resistance during MFC acclimation improved the anode performance mainly by diminishing the R_{CT}, which impacted the overall kinetics of anodic acetate oxidation, and thus reduced the overall electrode resistance. At the most positive anode potential of −115 mV, R_{CT} with 20 Ω was 31% lower than that with 50 Ω while R_d decreased by only 18%. Thus, decreasing R_{ext} during acclimation favored the anode kinetics to a greater extent than diffusional resistances, likely due to the adaptation of the microbial biofilm to stressful conditions produced by the higher current densities and a consequently lower localized pH, which will occur when using smaller resistances that produce higher anode potentials.

Diminishing the overall anode resistance can improve the reactor performance by reducing the reactor internal resistance. However, the total impact of a reduced anode resistance will only be reflected in overall performance if the anode resistance is an appreciable fraction of the internal resistance. The overall internal resistance of an MFC is a function of the sum of the anode, cathode, and solution resistances (Rossi et al., 2019). Thus, reducing only R_{An} may not significantly improve the performance of the MFC if most of the internal resistance is dominated by the cathode or solution resistances. Maximum power density in MFCs could be improved only by a simultaneously reduction of anode, cathode, and solution resistances by designing more compact reactors and favoring proton transport between anode and cathode to avoid the development of pH imbalances and the comparison of mass-transfer limitations in the anodic reaction.

4. Conclusions

Reducing R_{ext} during MFC acclimation decreased R_{CT} and R_d based on an EIS analysis. With R_{ext} of 20 Ω the charge transfer and diffusion resistances were lower with respect to those obtained with 50 Ω. The smaller R_{CT} and R_d at 20 Ω decreased the overall anode resistance from 7.0 ± 0.1 mΩ m^2 (50 Ω R_{ext}) to 5.13 ± 0.02 mΩ m^2 (20 Ω R_{ext}), and increased the peak current densities from 21 ± 0.4 A m^{-2} (50 Ω R_{ext}) to 29 ± 1 A m^{-2} (20 Ω R_{ext}).

CRediT authorship contribution statement

Ruggero Rossi: Conceptualization, Formal analysis, Writing - original draft. **Bruce E. Logan:** Conceptualization, Funding aquisition, Writing - review & editing.

Declaration of Competing Interest

The authors declare that they have no known competing financial interests or personal relationships that could have appeared to influence the work reported in this paper.

Acknowledgements

The authors acknowledge funding by the Environmental Security Technology Certification Program via cooperative research agreement W9132T-16-2-0014 through the US Army Engineer Research and Development Center, and funding by the Pennsylvania State University.

Appendix A. Supplementary data

Supplementary data to this article can be found online at https://doi.org/10.1016/j.biortech.2020.123921.

References

Bisquert, J., Garcia-Belmonte, G., Fabregat-Santiago, F., Bueno, P.R., 1999. Theoretical models for AC impedance of finite diffusion layers exhibiting low frequency dispersion. J. Electroanal. Chem. 475, 152–163. https://doi.org/10.1016/S0022-0728(99)00346-0.

Bond, D.R., Strycharz-Glaven, S.M., Tender, L.M., Torres, C.I., 2012. On electron transport through geobacter biofilms. ChemSusChem 5, 1099–1105. https://doi.org/10.1002/cssc.201100748.

Brug, G.J., van den Eeden, A.L.G., Sluyters-Rehbach, M., Sluyters, J.H., 1984. The analysis of electrode impedances complicated by the presence of a constant phase element. J. Electroanal. Chem. 176, 275–295. https://doi.org/10.1016/S0022-0728(84)80324-1.

Cario, B.P., Rossi, R., Kim, K.Y., Logan, B.E., 2019. Applying the electrode potential slope method as a tool to quantitatively evaluate the performance of individual microbial

electrolysis cell components. Bioresour. Technol. 287, 121418. https://doi.org/10.1016/j.biortech.2019.121418.
Cheng, S., Xing, D., Call, D.F., Logan, B.E., 2009. Direct biological conversion of electrical current into methane by electromethanogenesis. Environ. Sci. Technol. 43, 3953–3958. https://doi.org/10.1021/es803531g.
Dominguez-Benetton, X., Sevda, S., Vanbroekhoven, K., Pant, D., 2012. The accurate use of impedance analysis for the study of microbial electrochemical systems. Chem. Soc. Rev. 41, 7228–7246. https://doi.org/10.1039/c2cs35026b.
Dykstra, J.E., Biesheuvel, P.M., Bruning, H., Ter Heijne, A., 2014. Theory of ion transport with fast acid-base equilibrations in bioelectrochemical systems. Phys. Rev. E 90, 1–10. https://doi.org/10.1103/PhysRevE.90.013302.
Feng, Y., Yang, Q., Wang, X., Logan, B.E., 2010. Treatment of carbon fiber brush anodes for improving power generation in air-cathode microbial fuel cells. J. Power Sources 195, 1841–1844. https://doi.org/10.1016/j.jpowsour.2009.10.030.
Hong, Y., Call, D.F., Werner, C.M., Logan, B.E., 2011. Adaptation to high current using low external resistances eliminates power overshoot in microbial fuel cells. Biosens. Bioelectron. 28, 71–76. https://doi.org/10.1016/j.bios.2011.06.045.
Jung, S., Regan, J.M., 2011. Influence of external resistance on electrogenesis, methanogenesis, and anode prokaryotic communities in microbial fuel cells. Appl. Environ. Microbiol. 77, 564–571. https://doi.org/10.1128/AEM.01392-10.
Logan, B.E., 2009. Exoelectrogenic bacteria that power microbial fuel cells. Nat. Rev. Microbiol. 7, 375–381. https://doi.org/10.1038/nrmicro2113.
Logan, B.E., Rossi, R., Ragab, A., Saikaly, P.E., 2019. Electroactive microorganisms in bioelectrochemical systems. Nat. Rev. Microbiol. 17, 307–319. https://doi.org/10.1038/s41579-019-0173-x.
Logan, B.E., Zikmund, E., Yang, W., Rossi, R., Kim, K.-Y., Saikaly, P.E., Zhang, F., 2018. Impact of ohmic resistance on measured electrode potentials and maximum power production in microbial fuel cells. Environ. Sci. Technol. 52, 8977–8985. https://doi.org/10.1021/acs.est.8b02055.
Lyon, D.Y., Buret, F., Vogel, T.M., Monier, J.M., 2010. Is resistance futile? Changing external resistance does not improve microbial fuel cell performance. Bioelectrochemistry 78, 2–7. https://doi.org/10.1016/j.bioelechem.2009.09.001.
Popat, S.C., Ki, D., Rittmann, B.E., Torres, C.I., 2012. Importance of OH^- transport from cathodes in microbial fuel cells. ChemSusChem 5, 1071–1079. https://doi.org/10.1002/cssc.201100777.
Rossi, R., Cario, B.P., Santoro, C., Yang, W., Saikaly, P.E., Logan, B.E., 2019. Evaluation of electrode and solution area-based resistances enables quantitative comparisons of factors impacting microbial fuel cell performance. Environ. Sci. Technol. 53, 3977–3986. https://doi.org/10.1021/acs.est.8b06004.
Rossi, R., Hall, D.M., Wang, X., Regan, J.M., Logan, B.E., 2020. Quantifying the factors limiting performance and rates in microbial fuel cells using the electrode potential slope analysis combined with electrical impedance spectroscopy. Electrochim. Acta 348, 136330. https://doi.org/10.1016/j.electacta.2020.136330.
Rossi, R., Logan, B.E., 2020. Unraveling the contributions of internal resistance components in two-chamber microbial fuel cells using the electrode potential slope analysis. Electrochim. Acta 348, 136291. https://doi.org/10.1016/j.electacta.2020.136291.
Torres, C.I., Krajmalnik-Brown, R., Parameswaran, P., Marcus, A.K., Wanger, G., Gorby, Y.A., Rittmann, B.E., 2009. Selecting anode-respiring bacteria based on anode potential: phylogenetic, electrochemical, and microscopic characterization. Environ. Sci. Technol. 43, 9519–9524. https://doi.org/10.1021/es902165y.
Torres, C.I., Marcus, A.K., Rittmann, B.E., 2008. Proton transport inside the biofilm limits electrical current generation by anode-respiring bacteria. Biotechnol. Bioeng. 100, 872–881. https://doi.org/10.1002/bit.21821.
Watson, V.J., Logan, B.E., 2011. Analysis of polarization methods for elimination of power overshoot in microbial fuel cells. Electrochem. Commun. 13, 54–56. https://doi.org/10.1016/j.elecom.2010.11.011.
Yang, G., Huang, L., Yu, Z., Liu, X., Chen, S., Zeng, J., Zhou, S., Zhuang, L., 2019. Anode potentials regulate Geobacter biofilms: New insights from the composition and spatial structure of extracellular polymeric substances. Water Res. 159, 294–301. https://doi.org/10.1016/j.watres.2019.05.027.
Zhang, X., He, W., Ren, L., Stager, J., Evans, P.J., Logan, B.E., 2015. COD removal characteristics in air-cathode microbial fuel cells. Bioresour. Technol. 176, 23–31. https://doi.org/10.1016/j.biortech.2014.11.001.
Zhou, D.B., Poorten, H.V., 1995. Electrochemical characterisation of oxygen reduction on teflon-bonded gas diffusion electrodes. Electrochim. Acta 40, 1819–1826. https://doi.org/10.1016/0013-4686(95)00109-R.
Zhu, X., Tokash, J.C., Hong, Y., Logan, B.E., 2013. Controlling the occurrence of power overshoot by adapting microbial fuel cells to high anode potentials. Bioelectrochemistry 90, 30–35. https://doi.org/10.1016/j.bioelechem.2012.10.004.
Zhu, X., Yates, M.D., Hatzell, M.C., Ananda Rao, H., Saikaly, P.E., Logan, B.E., 2014. Microbial community composition is unaffected by anode potential. Environ. Sci. Technol. 48, 1352–1358. https://doi.org/10.1021/es404690q.